HOW RELIABLE ARE PREDICTION AND MEASUREMENT OF WELD RESIDUAL STRESSES? LESSONS FROM THE NET NETWORK.

M C SMITH*, V AKRIVOS* and A VASILEIOU*

** The University of Manchester, Oxford Road, Manchester, M13 9PL, United Kingdom, mike.c.smith@manchester.ac.uk*

DOI 10.3217/978-3-85125-615-4-18

ABSTRACT

The Task Groups of the NeT European Network undertake closely controlled round robin studies examining the prediction and measurement of residual stresses in thoroughly characterised welded benchmarks. Task Groups 4 and 6 are examining three-pass slot welds in plates made from AISI316L(N) and Alloy 600 respectively. A very large body of independent RS measurements and simulations have been performed, giving a unique insight into the real-world reliability of both RS measurements and finite element simulation of welding. This paper reviews NeT Task Groups 4 and 6, and considers their implications for modelling of welding processes.

INTRODUCTION

Finite element methods are used increasingly to predict weld residual stresses for use in weld structural performance assessments [1-3], since they offer the prospect of more accurate, less conservative residual stress profiles than the upper bound profiles currently provided in structural integrity assessment procedures such as R6 [4] and API 579 [5]. However, the potential uncertainties in finite element predictions remain a serious concern. The R6 structural integrity assessment procedure used in the UK includes guidelines for finite element prediction of weld residual stresses [6, 7] and imposes strict validation requirements on those predictions. The level of validation required depends on the structural integrity significance of weld residual stresses in the weldment being considered, but wholly unvalidated finite element predictions may not be used in structural integrity assessments.

Continuum-mechanics-based finite element prediction of the welding process is sometimes considered as a relatively straightforward “engineering” technique, with the attention of researchers focussed on modelling of sub-continuum features such as microstructure development in the weld pool and the adjacent strain/heat affected zone. However, the forcing functions for the development of such meso-scale features are the

transient thermal and stress-strain fields developed during welding. Accurate continuum level modelling of the welding process is thus a pre-requisite for useful modelling at lower length-scales.

The mission of the European Network on Neutron Techniques Standardization for Structural Integrity (NeT) is to develop experimental and numerical techniques and standards for the reliable characterisation of residual stresses in structural welds. NeT was first established in 2002. It involves over 30 organisations from Europe and beyond. NeT operates on a "contribution in kind" basis from industrial, academic, and research facility partners. Each problem examined by the network is tackled by creating a dedicated Task Group (TG), which undertakes measurement and modelling studies and the interpretation of the results. Since its formation, NeT has examined a number of benchmark weldments, of steadily increasing complexity.

NeT TG1 [8-23] examined a single weld bead laid onto the surface of an AISI 316L austenitic steel plate. AISI 316L is normally considered a "simple" material to model: no solid-state phase transformation takes place at temperatures relevant to the development of residual stresses and distortion, so there is normally assumed to be no need to model microstructure development as part of the process of predicting the weld residual stress state. This weld geometry produced a strongly three-dimensional residual stress distribution, with similar characteristics to a weld repair, and proved to be very challenging to simulate accurately.

NeT TG4 [24-33] was designed as a natural follow-on to TG1, using similar material (AISI 316L(N)), but with the single weld bead of TG1 replaced by three superimposed weld beads laid into a slot. It introduced a multi-pass weld and a significant volume of weld metal, while retaining the portability of TG1. Participants in TG4 were set the following challenges:

- To make accurate measurements of residual stress in weld metal, where grain size and microstructural texture make diffraction-based measurements difficult. The volume of weld metal in TG1 was so limited that the residual stress field could be largely characterised without attempting to make measurements in the weld itself.
- To extend the line-based residual stress measurements made in TG1 to full 3D spatial mapping of the residual stress field.
- To improve statistical descriptions of measured stresses, and thereby reduce uncertainty and provide reliable validation targets for residual stress predictions.
- To make accurate predictions of the development of material properties and the final residual stress field in weld metal, which starts life molten, and in the adjacent heat/strain affected zone which, like weld metal, undergoes multiple high temperature thermo-mechanical cycles.

NeT TG4 largely succeeded in these objectives, and the project is probably the most detailed and extensive study on weld residual stress simulation and measurement yet carried out.

NeT TG5 [34, 35] examined the prediction and measurement of residual stresses in a material that undergoes both bainitic and martensitic solid state phase transformations during welding, the low alloy steel SA508 Gr 3 Cl 1. The TG5 benchmark is a simple beam specimen with a single autogenous weld bead laid along one edge. Two different welding speeds are used, to promote either bainitic or martensitic structures in the fusion zone and HAZ.

NeT TG6, started most recently, in 2012, examines the behaviour of Tungsten inert gas (TIG) welds made using nickel-based Alloy 82 filler on an Alloy 600 substrate, using a three pass slot weld geometry similar to the TG4 specimen. Residual stresses in welds made using Alloy 82 or Alloy 182 filler are of considerable interest because these alloys are susceptible to primary water stress corrosion cracking when used in pressurized water reactor primary circuit dissimilar metal welds. Considerable effort has been expended in the measurement and prediction of residual stresses in PWR DMW's [36-39], with mixed results. These may be attributed partly to the complexity of the weldments being examined, and partly to the difficulties associated with neutron diffraction measurements in nickel alloy weld metals. NeT TG6 thus addresses an important need: it allows a challenging material to be examined within the well-established NeT framework of detailed characterization of both the welding process and the materials used, multiple, diverse residual stress measurements, and extensive finite element simulation.

NeT TG6 has now reached a stage where sufficient results are available to allow assessment of the performance of measurement and simulation techniques. This paper thus reviews the outputs of the NeT TG4 and TG6 projects together, and considers their implications for the accuracy and reliability of finite element predictions of weld residual stresses in "simple" metal alloys, where explicit consideration of microstructure is not necessary in order to predict continuum stresses and distortions. It first briefly describes the design, manufacture and metallographic/microscopic characterisation of the benchmark specimens themselves, concentrating upon the information required to make and validate FE simulations, and then summarises the extensive mechanical testing campaigns that were undertaken to provide the materials data necessary for accurate simulation. The accuracy and reliability of the thermal simulations are then reviewed – accurate thermal simulation is a pre-requisite for any further modelling. The residual stress measurement camaigns are then reviewed, again to assess their accuracy and reliability, before examining the performance of the mechanical simulations.

THE NET TG4 AND TG6 BENCHMARK SPECIMENS

SPECIMEN DESIGN AND MANUFACTURE

TG4 specimens were fabricated from AISI 316L(N) plate, while TG6 specimens used Alloy 600 plate. Basic dimensions are shown in Figure 1. The specimen designs were intended to allow sufficient constraint to develop an intense three-dimensional residual stress field around a short multi-pass weld, while remaining easily portable, with a plate thickness that allowed full-field measurements of residual stress using diffraction-based methods, without excessive count times. The TG6 specimen is thinner than TG4, at 12mm rather than 18mm. The reduction in thickness was made to aid diffraction-based residual stress measurements, in what is known to be a challenging material. A completed TG4 specimen is shown in Figure 2, while Figure 3 shows a TG6 specimen prior to welding.

All TG4 specimens were fabricated from a single plate of AISI 316L(N) material, originally procured for the ITER fusion reactor project and donated to the NeT network. TG6 specimens were fabricated from two different heats of Alloy 600 plate.

Plate A material was used to fabricate production specimens, and for critical materials characterization testing. ***Plate B*** material was used for the manufacture of trial specimens and initial materials characterization testing. A total of fifteen TG4 specimens were fabricated over the course of the project. Nine TG6 specimens have been fabricated from Plate A material so far.

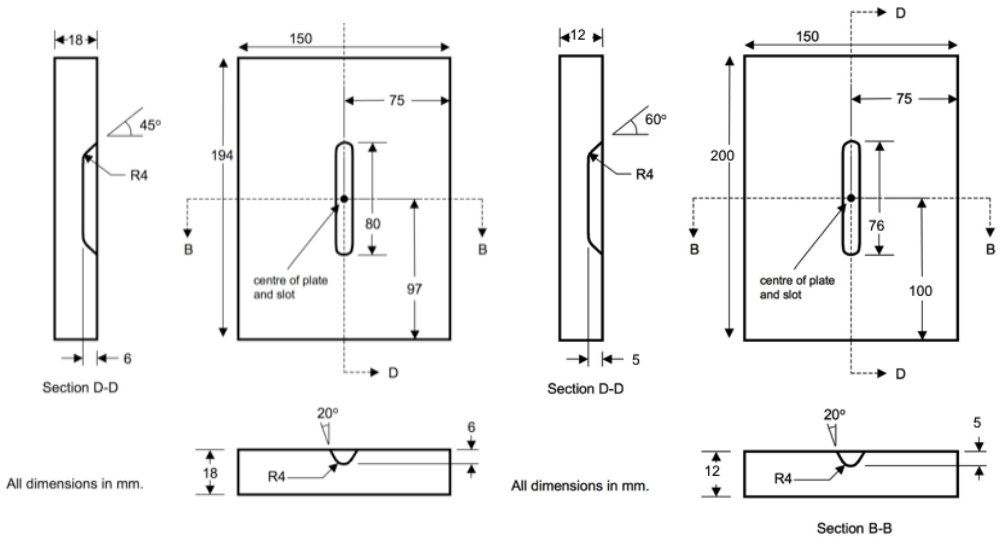

TG4 specimen TG6 specimen

Fig. 1 Dimensions of NeT TG4 and NeT TG6 benchmark specimens prior to welding. Note that line BD is a through-wall line at the centre of the plates, at the intersection of Sections B-B and D-D

Both benchmarks contain three superimposed weld passes deposited in a central slot using a tungsten inert gas (TIG) process, using AISI 316L filler in TG4 and Alloy 82 filler in TG6. A three-pass weld was selected for TG4, based upon knowledge of the cyclic hardening behaviour of AISI 316 steel. This is rapid, so three passes are sufficient to achieve significant hardening without placing an undue time burden on subsequent modelling. Alloy 600 is expected to cyclically harden slower than AISI 316, but the desire to maintain maximum commonality with TG6 led to a three-pass slot weld in TG6.

Weld parameters were developed for both benchmarks via a series of trials performed on additional multi-slot plates, using pedigree material for TG4, and on Plate B material for TG6, with the aim of developing processes that gave slight overfill in three passes without excessive heat input. Production welding for TG4 was performed using a programmable TIG welding machine. Full automation was not achieved, as the welding engineer retained control over the exact torch path and traverse length. The production weld parameters for TG6 were fully programmed into a welding robot to ensure repeatability. Table 1 summarises the steady-state weld process parameters for both benchmarks. Detailed process parameter records were kept, and these are reported elsewhere [32, 40]. It is evident that the heat inputs achieved in TG6 were higher than for TG4, especially in passes two and three.

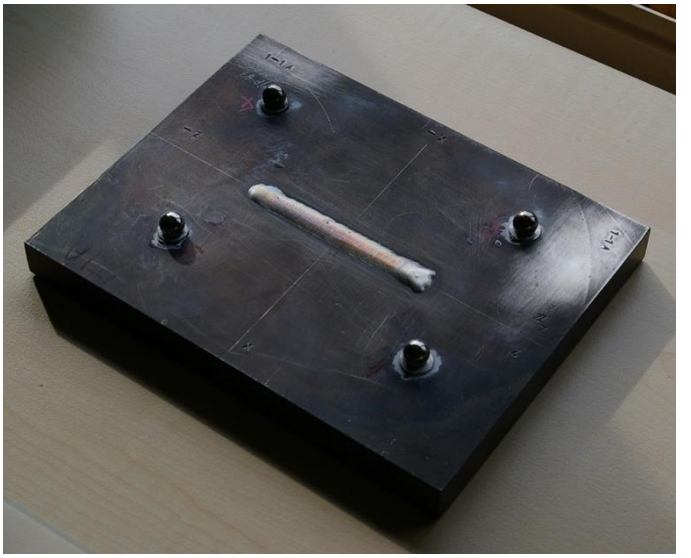

Fig. 2 Completed TG4 specimen prior to neutron diffraction measurements

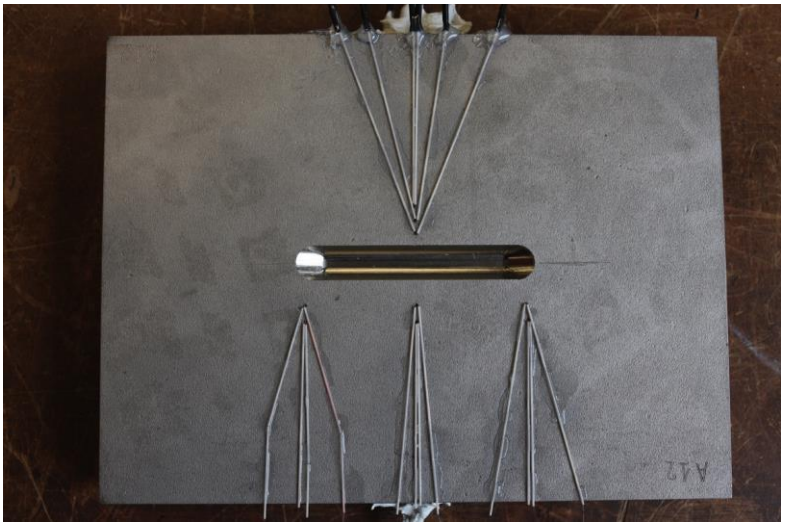

Fig. 3 TG6 specimen prior to welding, showing machined slot and top surface thermocouples

Table 1 Steady-state welding parameters at mid-length for TG4 and TG6 benchmarks

Benchmark	Pass	Mean current (A)	Mean voltage (V)	Traverse speed (mm/s)	HI (kJ/mm)
TG4	1	220	10	1.27	1.73
TG4	2	195	10	1.27	1.54
TG4	3	185	10	1.27	1.46
TG6	1	220	10.8	1.17	2.03
TG6	2	220	13.4	1.17	2.52
TG6	3	220	12.3	1.17	2.31

TRANSIENT TEMPERATURES DURING WELDING

Surface-mounted thermocouple arrays were used to monitor transient temperatures during welding. The array design philosophy for both benchmarks was the same: a redundant, symmetric array at mid-length where the welding temperature transient response is expected to be quasi-steady-state, positioned in the far field where the thermocouples respond as if the weld torch/pool is a point heat source; and additional thermocouple arrays at the slot ends to record the three-dimensional temperature transients there. The thermocouple locations are shown in Figure 4. K-type thermocouples were used. Three TG4 plates were instrumented, with the thermocouples spot-welded to the plate surface. All the TG6 plates were instrumented, with an attachment technique that aimed to learn lessons from TG4 and improve thermocouple accuracy and reliability (see Figure 2)[1].

Figure 5 shows the transient temperatures recorded at the lower surface thermocouples during pass 1 for seven TG6 specimens. The responses show good repeatability. The measured temperature rises at the mid-length thermocouple arrays are tabulated for TG4 in Table 2, and for TG6 in Table 3. Responses from symmetric thermocouples are grouped. We note:

- The temperature rises measured for TG6 are much greater than for TG4, a reflection of the higher heat inputs and the thinner plate. This is particularly evident on the back face, where the central thermocouple T9 records a peak temperature above 900ºC during pass 1. This is much greater than for TG4 (about 450ºC).
- The uncertainties in measured temperature rises are lower for TG6, due to both the improved attachment technique and the larger number of instrumented specimens.
- It appears to be necessary to instrument a number of nominally identical specimens with redundant, symmetric thermocouple arrays in order to make reliable measurements of the transient temperature fields.

Separate, single TG4 and TG6 specimens were instrumented with two buried thermocouple arrays each. The buried arrays were designed to allow optimization of local

[1] The thermocouple wires were encased in protective sheaths, the junctions were spot welded into shallow dimples machined into the plate surface, and the top surface arrays were protected with insulating paste to prevent errors due to arc shine.

weld heat source parameters such as size, shape, and flux distribution. Details are given elsewhere [32, 40].

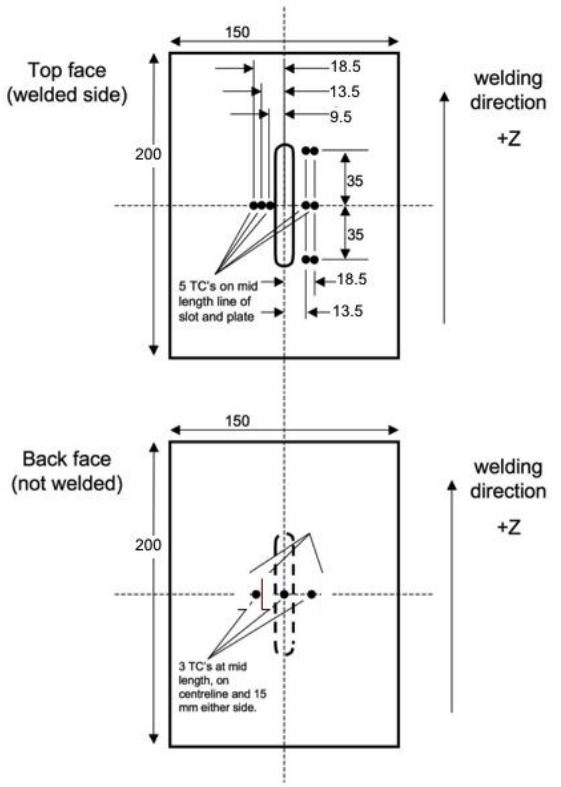

Fig. 4 Locations of surface-mounted thermocouples on NeT TG6 specimen (array design for TG4 was identical except top surface thermocouples were positioned at 9mm, 13mm, and 18mm from the weld centreline).

Table 2 Measured temperature rises at mid-length thermocouples for NeT TG4, from arrays on three welded plates

Thermocouple group	Nominal lateral position |x|	Mean measured temperature rise (°C) (+/-1 sd)		
		Pass 1	Pass 2	Pass 3
T10 (top)	9 mm	583.2 +/-35.3	604.0 +/-78.5	632.1 +/-155.7
T2, T11 (top)	13 mm	384.7 +/-31.6	358.9 +/-36.6	340.3 +/-42.8
T5, T12 (top)	18 mm	236.2 +/-17.4	206.2 +/-14.6	188.9 +/-16.8
T7, T8 (bottom)	15 mm	275.7 +/-10.7	225.7 +/-7.5	198.8 +/-8.1
T9 (bottom)	0	451.3 +/-3.4	346 +/-6.5	299.4 +/-4.0

Table 3 Measured temperature rises at mid-length thermocouples for NeT TG6, from arrays on seven welded plates (pass 1), and 4 plates (passes 2 and 3).

Thermocouple group	Nominal lateral position |x|	Mean measured temperature rise (°C) (+/-1 sd)		
		Pass 1	Pass 2	Pass 3
T10 (top)	9.5 mm	841.2 +/-34.2	932.2 +/-22.4	1004.1 +/-25.8
T2, T11 (top)	13.5 mm	540.7 +/-34.0	557.4 +/-12.4	607.2 +/-51.4
T5, T12 (top)	18.5 mm	395.7 +/-14.6	394.1 +/-12.8	386.0 +/-11.2
T7, T8 (bottom)	15 mm	480.9 +/-18.6	468.3 +/-21.6	443.9 +/-22.0
T9 (bottom)	0	910.2 +/-18.5	789.5 +/-10.5	717.5 +/-11.2

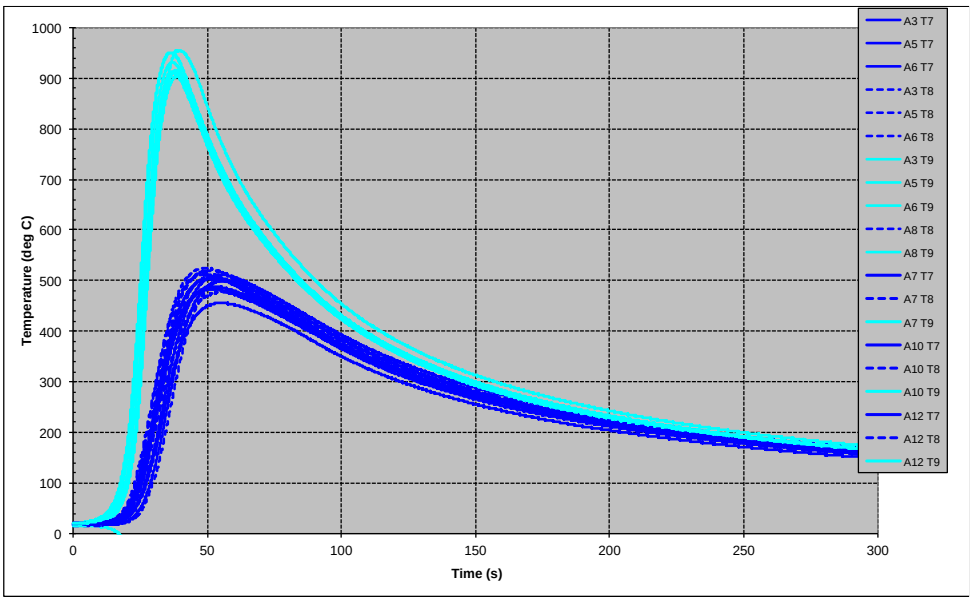

Fig. 5 measured transient temperatures for pass 1 at back face (lower surface) thermocouples for seven TG6 specimens

DISTORTION MEASUREMENTS

Distortion during welding was measured for both benchmarks. For TG4, a coordinate measuring machine was used to profile selected specimens before and after welding. The final deformed shapes of all TG6 specimens were measured using a hand-held laser scanner, while one specimen was measured prior to welding, at inter-pass conditions between each pass, and after completion of welding.

METALLOGRAPHIC CHARACTERISATION

The fusion boundary profile and melted area are key parameters for finite element weld models. Both TG4 and TG6 made use of multi-slot specimens containing welds with one,

two, and three passes which could be sectioned for metallography. The transverse cross-sections for TG4 are shown in Figure 6. AISI 316L(N) is considered a well-understood material for weld modelling. Neither excessive grain growth, nor re-crystallisation are expected in the heat/strain affected zone, and solid-state phase transformation is absent. Cyclic hardening leads to a steady increase in yield strength in the HAZ as the fusion boundary is approached and the plastic path length increases, and the weld metal used is closely matched to parent material [41]. Thus detailed microscopy was not performed as part of the NeT TG4 round robin.

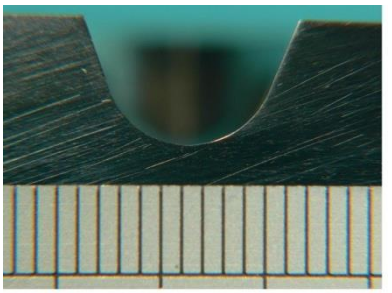

(a) Machined slot transverse profile

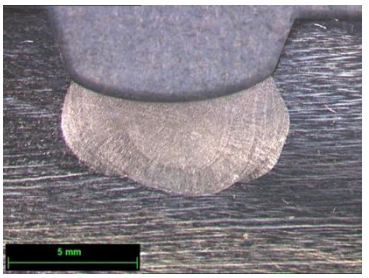

(b) Pass 1 weld bead transverse profile

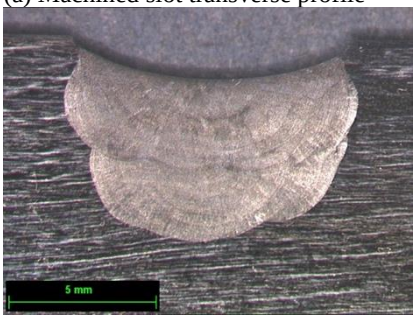

(c) Pass 1 and Pass 2 transverse fusion boundary profile

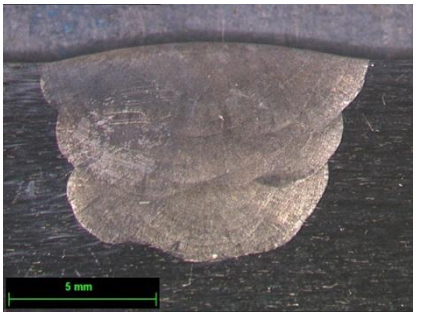

(d) Completed weld transverse fusion boundary profile

Fig. 6 Transverse fusion boundary profiles for passes 1, 2 and 3 in NeT TG4 AISI 316L(N) welded benchmark

Alloy 600 is a less well understood material for weld modelling, so more detailed microscopy was performed for TG6, comprising conventional polishing and etching to reveal the microstructure, hardness mapping, and electron back-scatter diffraction (EBSD) studies. Transverse macrographs are presented in Figure 7.

The Alloy 600 parent material has a bi-modal grain size distribution with large grains (100-500 μm) in a matrix of much smaller grains (tens of μm). The bi-modal distribution is clearly visible in the parent plate on the low magnification images in Figure 7a-c, and in a higher magnification image in Figure 7d. In contrast, the grain size in the Alloy 82 weld metal is significantly larger, with columnar grains close to the weld fusion boundaries and more equi-axed grains near the centre of the final weld bead. Individual columnar grains appear to span more than one weld bead. There is also a region of grain coarsening in the HAZ adjacent to the weld fusion boundary.

Crystallographic texture measurements were made on a sample extracted from a three pass TG6 weld. These revealed relatively weak texture in the parent material, and the bottom of the weld, but strong texture in the final weld bead.

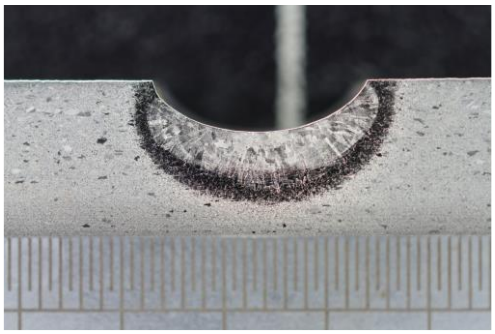

(a) Single pass weld

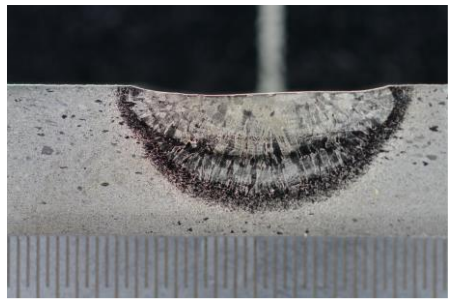

(c) Two pass weld

(c) Three pass weld

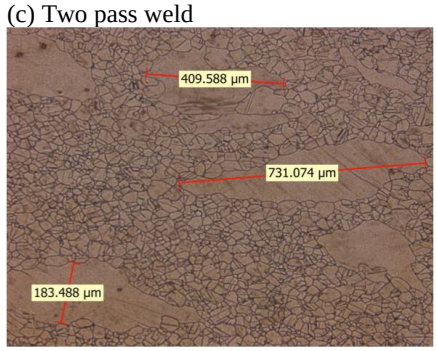

Alloy 600 parent plate (note high magnification)

Fig 7: Transverse fusion boundary profiles for passes 1, 2 and 3 and Alloy 600 parent plate grain morphology in NeT TG6 Alloy 600/82 welded benchmark

Vickers hardness maps for one-pass, two-pass and three-pass TG6 welds are presented in Figure 8. They reveal that the Alloy 82 weld metal and the coarse-grained region of the HAZ are significantly softer than the parent plate. There is also evidence of progressive cyclic hardening in parent material beneath the weld, and to a lesser extent in weld metal, plus a thin zone of hardened material near the surface of the plate. The latter is probably a result of the plate forming operations, as the upper and lower surfaces of the plate were left un-machined prior to welding.

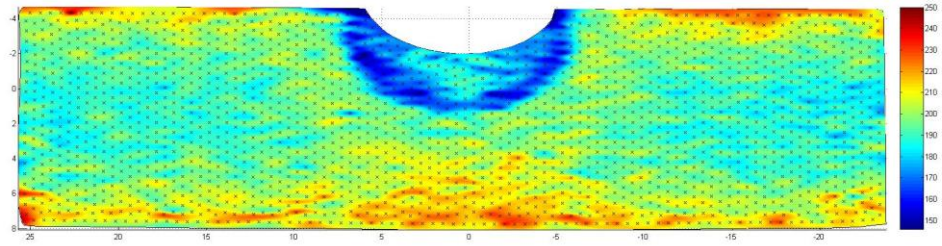

(a) Single pass weld

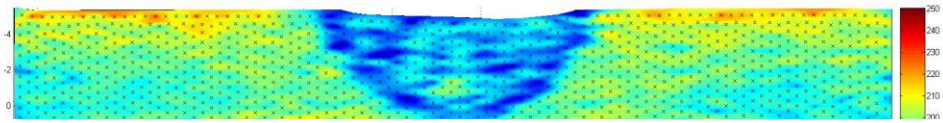

(b) two-pass weld

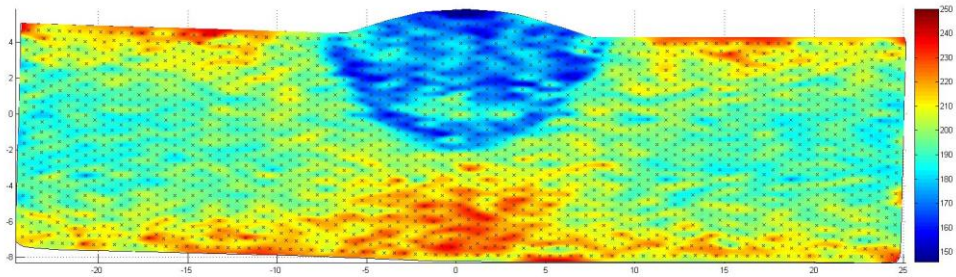

(c) three-pass weld

Fig 8: Vickers hardness variation on transverse planes in 1, 2 and 3-pass NeT TG6 Alloy 600/82 welded benchmarks, showing cyclic hardening in parent ligament, and softening in CGHAZ and under-matched weld metal.

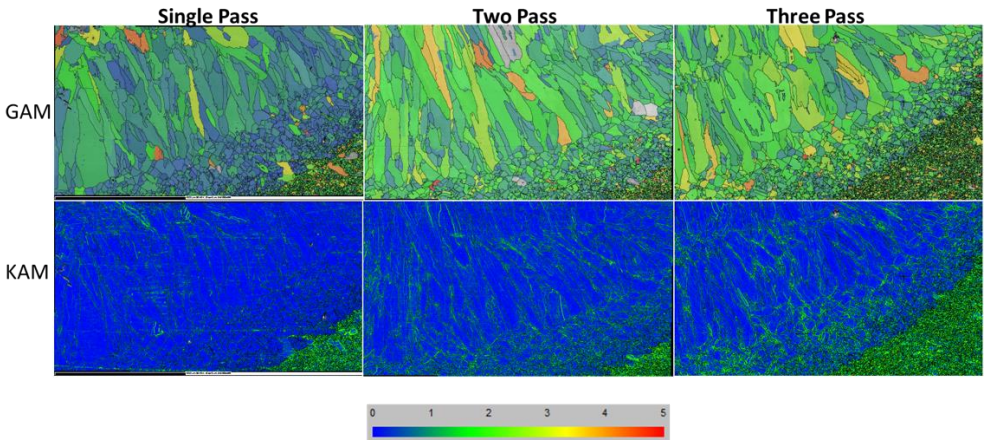

Fig 9: Qualitative mapping of the accumulated plastic strain in the pass 1 weld and HAZ of one, two, and three pass NeT TG6 benchmark welds using (top) grain average misorientation and (bottom) kernel average misorientation EBSD metrics. The low levels of misorientation in the coarse grained HAZ and wled metal are clearly visible, especially in the single pass weld.

Figure 9 presents EBSD maps of crystallographic misorientation made using two common metrics. Both show very clearly the low misorientation in the coarse-grained region of the HAZ and the columnar fusion zone of a single pass weld, compared with adjacent parent material, and the subsequent increase in misorientation as successive passes are deposited on top of each other. The EBSD data thus show very similar trends to the conventional hardness maps.

They Alloy 600/82 combination thus appears to show significant differences to AISI 316 in the weld and HAZ regions.

MATERIALS CHARACTERISATION

Materials characterisation performed for both TG4 and TG6 was focussed upon providing data over a full range of temperature sufficient to allow temperature-dependent mixed isotropic-kinematic hardening models to be derived for both constituents of each benchmark. If started from scratch this would be an onerous task, so maximum possible use was made of existing material property databases held by NeT participants, especially EDF Energy in the UK. New characterisation tests concentrated on gaps in existing data.

NET TG4

The AISI 316L(N) plate used for NeT TG4 has very similar physical and mechanical properties to the plate previously used for NeT TG1. The materials testing performed to support TG4 thus concentrated on the monotonic tensile and isothermal cyclic behaviour for both the parent AISI 316L(N) plate and the AISI 316L TIG weld metal. All other materials data were obtained from the database assembled for NeT TG1. A detailed materials compendium was compiled, comprising approximately 180Mb of test data.

Thermal and physical properties were assumed to be identical to those of the AISI 316L plate and TIG weld metal used for NeT TG1. Those in turn were derived from internal material properties databases held by NeT members, especially EDF Energy [32].

Only room temperature monotonic tensile tests were performed on the TG4 AISI 316L(N) material. These revealed behaviour very similar to the NeT TG1 material, so TG1 data obtained at temperatures up to 750ºC were also supplied to participants in NeT TG4. These detailed test data were supplemented by simplified proof stress vs. temperature data derived for TG1 that extended up to the melting point of 1400ºC [32].

EDF Energy have performed monotonic tensile testing on ER316L TIG weld metal made using welding wire of the same specification used for TG4, although not the same batch. Several different processing histories were used to produce weld metal suitable for testing, namely:

- Material extracted from a multi-pass weld pad, and tested in the as-welded condition
- Material extracted from a multi-pass weld pad, and tested after solution heat treatment
- Material extracted from two-pass welds laid into grooves (the minimum number of passes that produced sufficient weld cross-sectional area to manufacture test specimens), and tested in the as-welded condition
- Material extracted from the same two-pass welds, and tested after solution heat treatment

The processing history has a marked effect upon the tensile properties of weld metal, discussed in detail elsewhere [29]. It was judged that solution-treated 2-pass material offers the best facsimile of unhardened, just-deposited weld metal, and these data were therefore provided to TG4 participants, both as simplified proof stress vs. temperature data, and as full stress-strain responses.

AISI 316L cyclically hardens strongly, and its mechanical behaviour during welding is best described using mixed isotropic-kinematic material hardening models [42, 43]. Isothermal cyclic test data are required to fit the parameters in mixed hardening models. Cyclic testing was performed on both the parent plate material and on solution-treated two-pass TIG weld metal. The test parameters (strain rate and strain range), were chosen to be relevant to the expected response during welding, using the recommendations in the weld modelling guidelines incorporated into the R6 structural integrity assessment procedure [4, 7]. Testing extended up to 700ºC, above which AISI 316L ceases to cyclically harden.

NET TG6

The NeT TG6 specimen is fabricated from two materials, Alloy 600 plate and Alloy 82 weld metal. This material combination results in an under-matched weld. The presence of both an under-matched weld and possible softening in the HAZ make the mechanical behavior of NeT TG6 significantly different to the NeT TG4 AISI 316L(N) benchmark. In particular, treating weld and parent material as identical is not a good assumption. It was judged that the evolutionary hardening behavior of the alloy 82 weld metal would best be evaluated by testing solution-treated weld metal, a similar conclusion to that reached for NeT TG4.

Both Alloy 600 and Alloy 82 cyclically harden in a broadly similar manner to austenitic stainless steels, although at slower initial rates, albeit with a greater change between cycle 1 and saturation.

A further complication for NeT TG6 is the heat-to-heat variation in yield strength between Plate A and Plate B material. Most of the material available for characterization at the beginning of the project was from plate B. This required adjustment before use in simulation of the welded specimens made from Plate A material.

A large body of testing was performed, comprising:

- Thermo-physical property measurements for the Alloy 600 plate material
- Monotonic and isothermal cyclic testing of Plate B material in conventional testing machines over a range of temperatures up to 700ºC
- Monotonic and isothermal cyclic testing of Plate A material in conventional testing machines over a range of temperatures
- Thermo-mechanical testing of Plate A material in a Gleeble thermo-mechanical simulator
- Manufacture of a multi-pass weld pad from Alloy 82 weld metal
- Monotonic and isothermal cyclic testing of solution-treated Alloy 82 material in conventional testing machines over a range of temperatures up to 700ºC
- Thermo-mechanical testing of alloy 82 material in a Gleeble thermo-mechanical simulator

This testing supplemented data already available from other sources, in particular testing performed on material from an Alloy 182 weld pad by EDF Energy. Alloy 182 is the manual metal arc filler metal equivalent to alloy 82 wire, and data from these tests were used in Phase 1 simulations for the TG6 benchmark. In total, the TG6 characterisation programme was intended to provide the necessary mechanical properties data to allow the fitting of both conventional and visco-plastic Lemaitre-Chaboche mixed hardening models.

ORGANISATION OF MEASUREMENT AND SIMULATION ROUND ROBINS

The measurement and simulation round robins for both TG4 and TG6 were carried out independently and in parallel. Each was controlled by its own protocol. The protocol documentation was extensive and detailed:

- The measurement protocols specified where to measure, how to measure and what to report.
- The simulation protocols comprised the protocol itself (which specifies the conduct, reporting and accuracy targets for the analyses), and supporting manufacturing case histories and material properties compendia.

The TG4 measurement round robin commenced in 2009, and the reported measurements include high energy synchrotron X-ray diffraction measurements made on two specimens at the European Synchrotron Radiation Facility in Grenoble, neutron diffraction measurements performed at eight different facilities (including several re-measurements), deep hole drilling and incremental deep hole drilling measurements on two specimens, transverse and longitudinal contour method measurements on a number of specimens, and ultrasonic measurements. This is believed to be the largest measurements database ever developed on a welded benchmark specimen. The diffraction measurements database is

large enough to generate reliable mean profiles, to identify clear outliers, and to establish that there is no statistically significant difference in the residual stress field in the two specimens used for most of the non-destructive measurements.

The TG6 measurement round robin commenced in 2015. To date, neutron diffraction measurements have been performed at five different facilities. All measurements to date have been performed on the same specimen. One contour method measurement has been carried out with others planned, and incremental deep hole drilling measurements have been performed on a single specimen.

The TG4 simulation round robin also commenced in 2009. This was performed in two phases. In Phase 1, participants were first required to validate their thermal simulations of welding by matching the measured thermocouple responses and weld fusion boundary profiles, in order to demonstrate that the thermal load was essentially correct before proceeding to any mechanical analyses. The mechanical analyses were then performed using only materials data for the AISI 316L(N) parent material, in effect assuming that weld and parent material behaved identically. A large body of weld-metal-specific materials data were assembled for Phase 2 simulations, which concentrated upon varying both the high temperature behaviour of both constituent materials, and on the most appropriate materials data and constitutive behaviour to assume for weld metal.

The TG6 simulation round robin commenced in 2015. This is also being performed in two phases. Phase 1 consists of thermal analyses, to be validated against the extensive database of transient measured temperatures, and mechanical analyses using the available materials data at an early stage in the project. In a departure from previous NeT practice, participants were supplied with both raw mechanical test data and recommended fitted parameters for Lemaitre-Chaboche mixed hardening models. These were based upon test data available at the time, namely cyclic isothermal testing on Plate B parent material, and on Alloy 182 weld metal. Additional materials data specific to the Plate A parent material and Alloy 82 weld metal has now been obtained, and will be supplied for the Phase 2 round robin, which has not yet commenced.

RESULTS

ACCURACY OF TEMPERATURE PREDICTION

An accurate thermal solution is a pre-requisite for any subsequent simulations, irrespective of the length scale involved. The thermal solution calibration procedure recommended for both TG4 and TG6 was the same: to employ moving volumetric heat sources (typically ellipsoidal gaussian or Goldak sources); to calibrate the global heat source parameters using the temperature rises recorded at far-field thermocouples, and to calibrate local heat source parameters using the fusion boundary profile data. In both round robins, the only unknown global parameter is the welding efficiency: the welding power, torch speed, path, and start-stop transients are all known. The number of local parameters needed to define the source shape depends upon the heat source adopted: examples include the three radii of a simple ellipsoidal gaussian source, the position of its centroid with respect to the deposited weld bead, its angular inclination, and weave characteristics, if any.

Target solution accuracies were imposed based upon experience gained in the NeT TG1 benchmark, and were similar for both TG4 and TG6:

- The predicted cross-sectional area of fused weld/parent metal at mid-length of each of the three beads should be within ± 20% of the mean measured fused area of the trial beads.
- The analysis should reproduce the observed mid-length transverse fusion boundary profiles.
- The predicted increases in temperature, $\Delta\theta$ = (θ_{peak} -θ_o), at mid-length thermocouple positions T5, T7, T8, T9, and T12 should agree with the mean measured increases, $\Delta\theta_{mean}$, to within 10%. Results from T5 and T12, and from T7 and T8, were combined, since these thermocouples are symmetrically arranged on opposite sides of the bead.
- Analysts should strive to achieve similar levels of agreement for the mid-length near-field thermocouples T2, T10 and T11, and for the thermocouple arrays at the start and stop ends

The performance of the finite element thermal predictions for TG4 is reviewed in detail in [31]. With some identified exceptions, all eight participants met the accuracy criteria, so that variations in the thermal solution could be discounted when accounting for variations in subsequent mechanical analyses. Figure 10 plots predicted and measured temperature histories for a pair of lower surface thermocouples. This emphasises the general quality of the thermal predictions.

A further accuracy measure is the overall RMS error for the mid-length thermocouple arrays, defined as:

$$Error_{RMS} = \sqrt{\frac{1}{n}\sum_{i=1}^{n}\left\{\frac{\left(q_{Ti,peak} - q_{Ti,0}\right) - \Delta q_{Ti,mean}}{\Delta q_{Ti,mean}}\right\}^2}$$

where θ is temperature, $\Delta\theta$ is temperature rise, the suffices *Ti* identify individual thermocouple locations, the suffix *mean* indicates mean measured data, and the suffices *0* and *peak* refer to FE predictions of initial and peak temperature respectively.

Table 4 presents sample RMS errors achieved for the NeT TG1, TG4 and TG6 round robins. We note:

- The TG1 thermal simulation was performed in two phases. As can be seen, the spread in predicted temperatures for the phase 1 simulations was large, with an RMS error of over 17%. It proved necessary to undertake a second thermal simulation campaign, in order to achieve acceptable agreement between simulations and between simulations and measurements, with an overall RMS error of 4.3% [14].
- Thermal solution performance in the TG4 round robin was much better, with an overall error over all simulations of 5.5%, which reduced to 3.7% when two participants submitted improved solutions and one solution with identified errors was removed [31]. The best simulation achieved an RMS error of 1.3%.
- A single TG6 simulation is reported, from the same team of researchers that achieved 1.3% error in TG4. The RMS error is somewhat higher, at 4.3%, but is

still at a level where the thermal solution is unlikely to contain serious errors, at least at weld mid-length.

It is important to remember that these low levels of solution error can only be achieved if the measured thermocouple data are accurate. In both TG4 and TG6, large amounts of data from different instrumented specimens and from equivalent thermocouples within individual specimens were combined to derive reliable target temperatures. If only limited thermocouple data are available, it is unlikely that they will be reliable enough to achieve these levels of assurance.

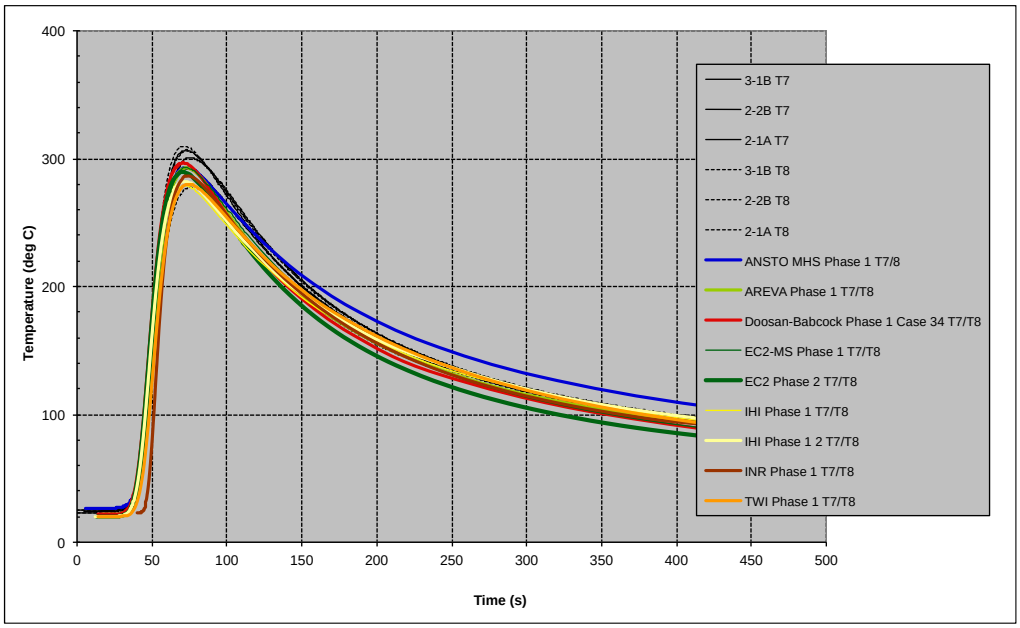

Fig. 10: Predicted and measured temperatures during pass 1 at thermocouples T7 and T8, lower surface mid-length, for NeT TG4 AISI316L(N) welded benchmark

Table 4 RMS errors in predicted temperature rises at mid-length thermocouple arrays for NeT TG1, TG4, and TG6 benchmarks, in all cases for the final weld pass

Benchmark	Analysis details	RMS error
TG1 single bead on plate, AISI 316L	Phase 1 round robin	17.2%
TG1 single bead on plate, AISI 316L	Phase 2 round robin	4.3%
TG4 3-pass slot weld, AISI 316L(N)	All simulations	5.5%
TG4 3-pass slot weld, AISI 316L(N)	“Phase 2”	3.7%
TG4 3-pass slot weld, AISI 316L(N)	Best simulation	1.3%
TG6 3-pass slot weld, Alloy 600/82	Best TG4 participant	4.3%

MEASUREMENT OF RESIDUAL STRESSES

NeT TG4

A large body of measured data was assembled for NeT TG4, see [30, 32]. Here we consider only results for a through-wall line at the centre of the specimen, identified as line BD (see Figure 1). This passes through all three weld beads, through the high temperature heat/strain affected zone, and through the remaining ligament, in a region where welding had achieved steady-state conditions, and where longitudinal variation in the residual stress field is small. Measured stresses in the longitudinal and transverse directions obtained using diffraction techniques are plotted in Figure 11, which shows:

- Individual measured data, with the uncertainties declared by the participating laboratory (usually, but not always, the fitting error for the raw diffraction peaks). The laboratories are anonymised, but the measured specimen is identified.
- The best-estimate measured profile, calculated using techniques originally developed in [23].
- An uncertainty of +/- one standard deviation on the best estimate.

The calculated uncertainties in the final best estimates are of order +/- 20 to 40 MPa. They are largest near free surfaces and in "pass 1" weld metal (weld metal with three thermo-mechanical load cycles). The final best-estimate profiles have very small normal stresses (not shown), which is as expected and an encouraging outcome. While this low level of final uncertainty is very encouraging, it is based upon analysis of a large dataset, and it is evident from Figure 11 that the uncertainty in individual measurements is higher.

Structural Integrity Assessment procedures such as R6 [4] recommend that residual stresses are measured using both diffraction and strain-relief methods, since they tend to have different characteristic errors. Good agreement between such independent techniques is deemed to be strong evidence of reliable measurements and helps negate the significant uncertainties associated with single measurement datasets.

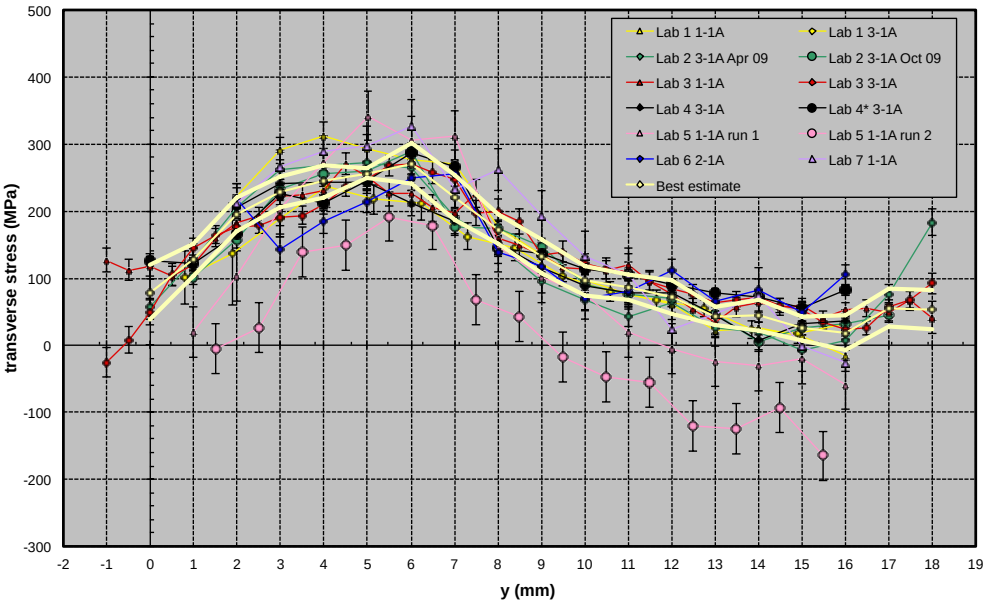

(a) transverse stress

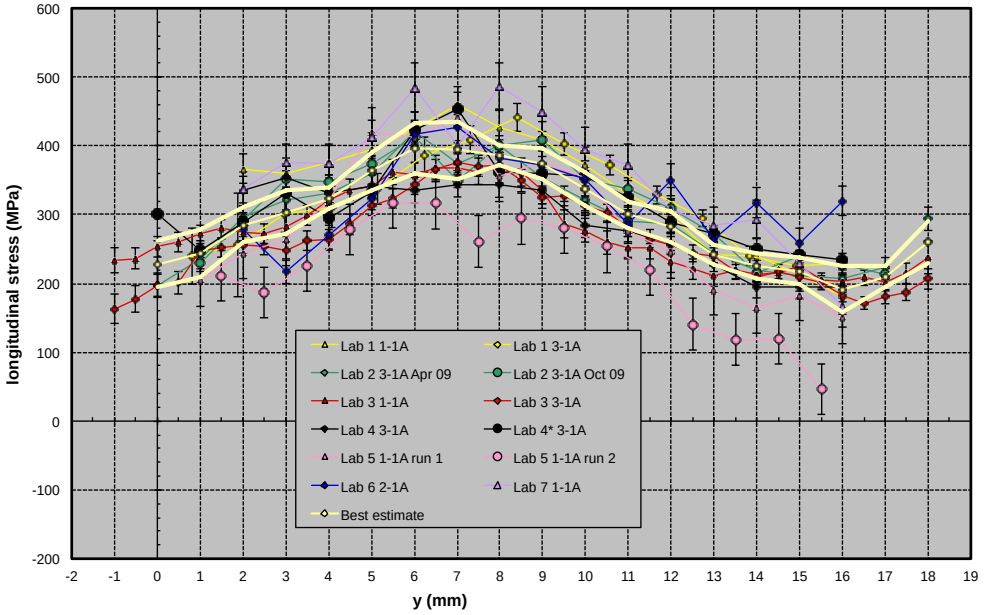

(b) longitudinal stress

Fig. 11: Residual stresses measured using diffraction methods on through-wall line BD in TG4 specimens. Best estimate and +/- 1 SD shown in yellow.

Both the contour method and the incremental deep hole drilling method were applied to NeT TG4. In both cases two specimens were measured. The measured longitudinal stresses on line BD are compared with the best estimate from diffraction-based measurements in

Figure 12. For both strain relief methods, one measurement agrees closely with the diffraction consensus, and one does not.

In the case of the contour measurements, the first measurement took no special precautions against the development of plasticity during the EDM cut. The contour method assumes that all deformation during the measurement process is elastic, so plastic deformation causes systematic errors in the measurement results. This measurement deviates from the diffraction-based best estimate (especially at other locations in the plate). The second measurement was optimized to minimize cut plasticity, and achieved good agreement with the diffraction consensus [44].

The incremental deep hole drilling technique is capable of returning accurate measured stresses when the residual stresses are high enough for plastic redistribution to occur during the measurement, so would be expected to have "worked" on line BD in TG4. Here, the first measurement returned visibly incorrect transverse stresses. No satisfactory explanation for this could be found, so the measurement was repeated on another specimen. As can be seen from figure 12, the second iDHD measurement agrees closely with the diffraction consensus.

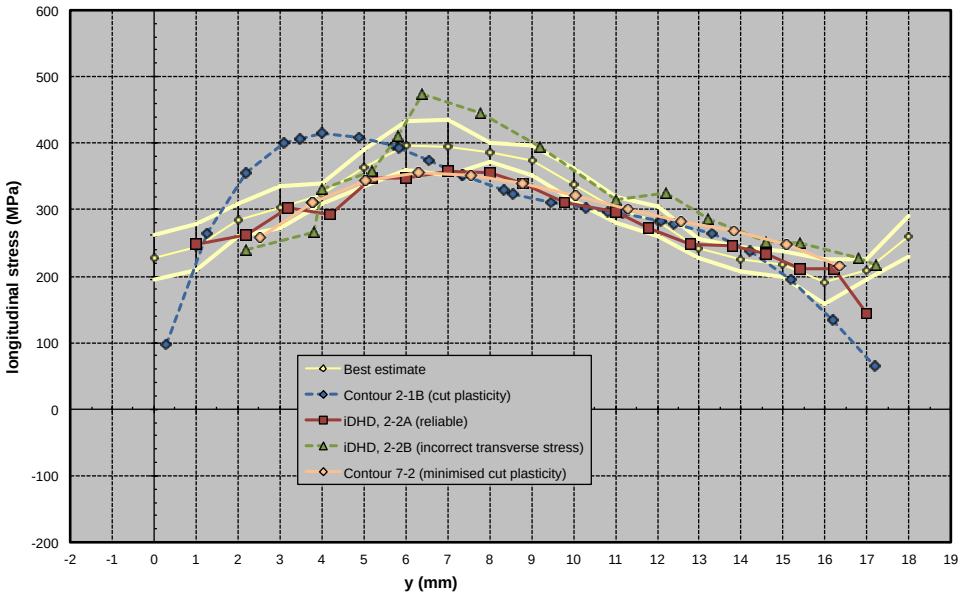

Fig 12: Comparison of measured longitudinal stresses on through-wall line BD in TG4 using strain relief methods with diffraction-based best estimates. Best estimate (with symbols and lines) and +/- 1sd (lines) shown in yellow.

NeT TG6

The measurement activities for NeT TG6 are not as complete as for TG4. The TG6 benchmark has proved to be a challenge for both diffraction-based and strain-based measurement methods. Neither the contour method nor deep hole drilling have yet yielded satisfactory results. The very large grain size and texture in Alloy 82 weld metal have

caused problems for neutron diffraction measurements, as has the large change in stress-free lattice parameter observed between Alloy 600 and Alloy 82.

Here we consider only the neutron diffraction measurements made at five facilities. Figure 13 plots measured stresses on line BD. These should be compared with stresses on the equivalent line in TG4 plotted in Figure 11. We note

- The through-wall distribution of stress in TG6 differs from that in TG4. Longitudinal stresses peak near the bottom surface in the parent ligament, with significantly lower stresses in weld metal and in the coarse-grained HAZ. In TG4, peak stresses develop in Pass 1 weld metal and the associated strain/heat affected zone. Transverse stresses peak near the middle of the plate, and fall near top and bottom surfaces, again in contrast to TG4.
- The uncertainties in measured stresses tend to be higher in TG6, especially in weld metal. This is probably due mostly to the difficulties in measuring in the TG6 material, especially in the weld, but the smaller data set may also be a factor, as may the much simpler technique used to generate a mean stress profile.

Clearly the combination of under-matched weld, softened HAZ, lower cyclic hardening rates, higher welding heat input, and thinner plate has led to a very different stress field in TG6 compared with the superficially similar TG4 benchmark.

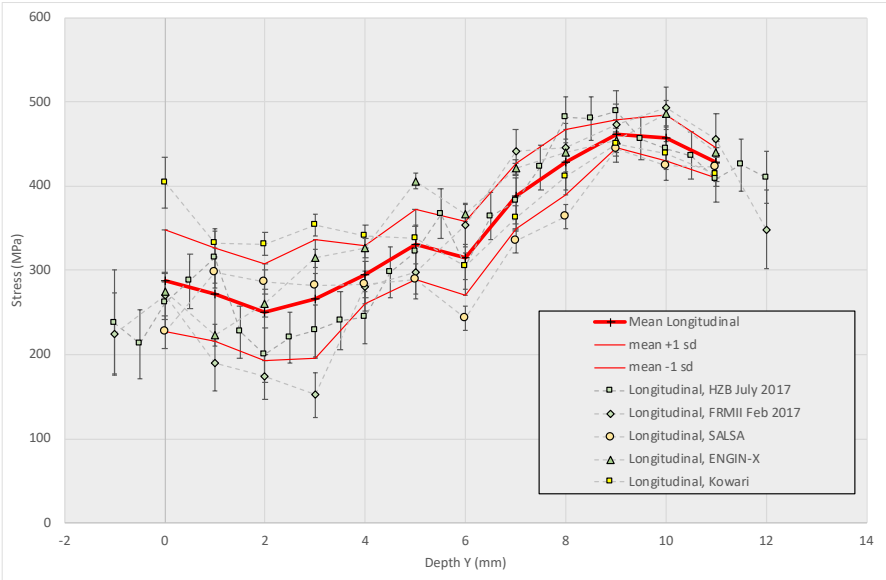

(a) Longitudinal stress

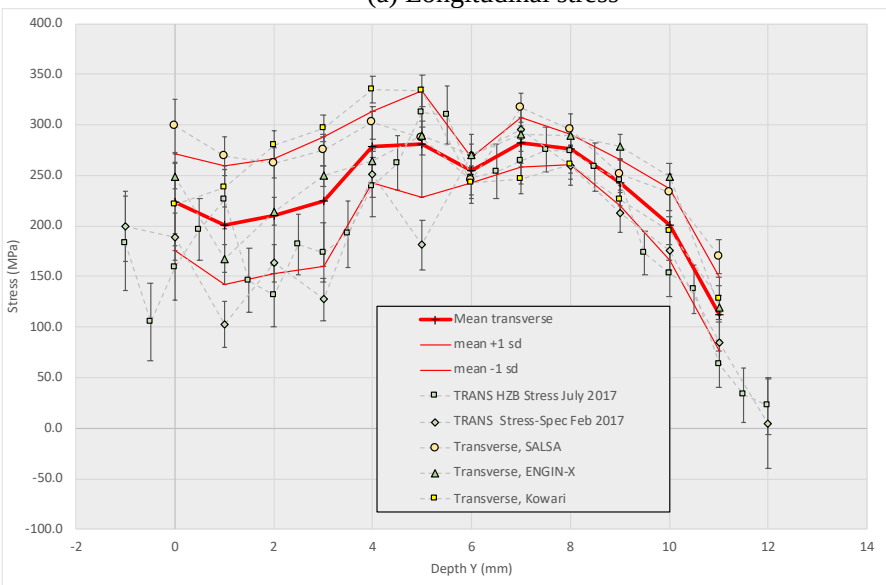

(b) Transverse stress

Fig. 13: Residual stresses measured using diffraction methods on through-wall line BD in TG6 specimen. Mean and +/- 1 SD shown in red

TG4

A total of eight organisations submitted 21 simulations as part of the main simulation round robin [30], with a further six simulations performed to examine details of weld metal hardening behaviour [29]. The stresses predicted on line BD by the main round-robin are compared with the measurement best estimate in Figure 14. At first sight the large spread in predictions is somewhat dispiriting, although not unexpected. The general picture is of "consensus plus outliers". The structural boundary conditions of the problem are well defined, and with a few known exceptions the thermal analyses are correct. Once analyses with known errors are identified and removed, then the most important source of error is the assumptions made about material hardening behaviour and about the mechanical properties of weld metal. Neither pure isotropic nor pure kinematic hardening are appropriate behaviours for AISI 316L(N): once these analyses are eliminated, the general accuracy improves greatly. The assumptions made about weld metal are also important: if weld metal properties are derived from tests on multi-pass weld metal or weld metal with any significant strain hardening, then stresses in the weld are over-predicted (in fact, the simple assumption that AISI 316L weld metal behaves like solution-treated parent material turns out to be remarkably good). A full description of the main simulation round robin and its performance is given in [30]

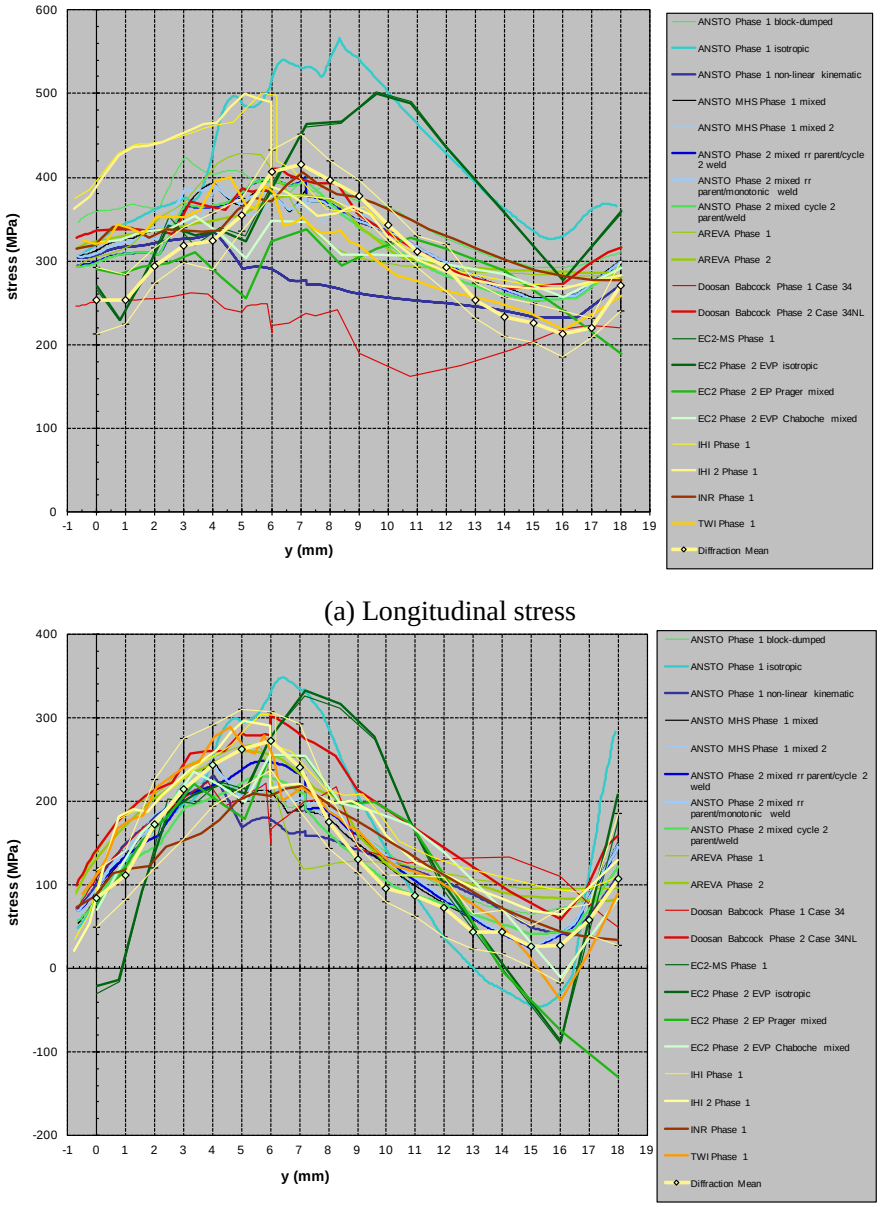

(a) Longitudinal stress

(b) Transverse stress

Fig. 14: Comparison of predicted and measured stresses in TG4 specimen on line BD, all main round robin analyses

The sensitivity studies reported in [29] made use of weld specific cyclic test data to fit Lemitre-Chaboche mixed hardening models for the weld metal in NeT TG4. These not only used test data from solution-treated 2-pass TIG welds (which effectively contain only a single weld bead because of remelting during the second pass), but also considered carefully both the initial "just solidified" yield strength, the cyclic hardening rate, and the final state of multi-pass weld metal, remembering that the thermo-mechanical cyclic

response of a steel will not necessarily be the same as its isothermal response. Figure 15 plots predictions from three of these fitted models, and compares them with the measured stresses on line BD (full details are in [29]). A high predictive accuracy is achieved, despite the analyses still using simple static plasticity with no viscous effects at high temperature other than a simple two-stage annealing functionality. This stops further isotropic hardening above a lower threshold temperature, and removes the hardening history completely at an upper limit temperature.

The sensitivity study results are probably at the limit of what can be achieved using conventional Lemaitre-Chaboche hardening models. They still retain unrealistic stress jumps associated both with changes in material model and with the simple annealing models used to eliminate hardening at high temperatures. Further improvements in predictive accuracy can probably only be achieved by explicit consideration of viscous effects at high temperatures, and a better understanding of thermo-mechanical hardening behaviour, especially in weld metal.

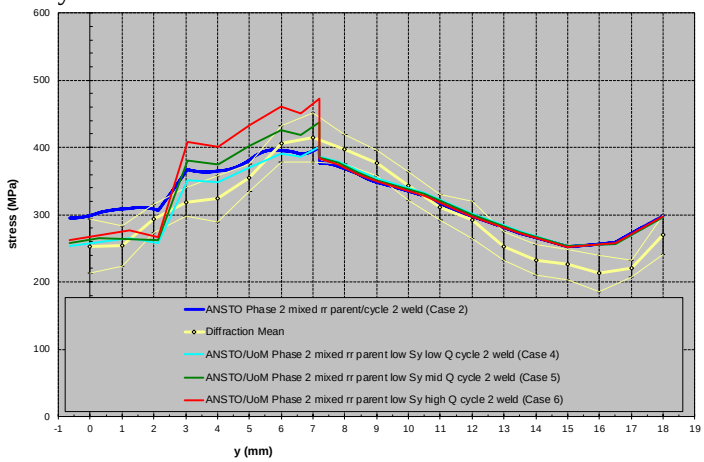

(a) longitudinal stress

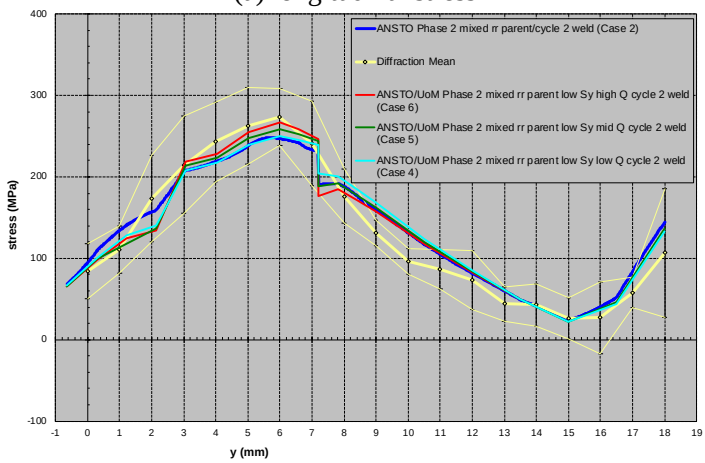

(b) Transverse stress

Fig. 15: Showing the impact of optimised mixed-hardening models for weld metal on predicted stresses on line BD in a TG4 specimen

TG6

The simulation work on NeT TG6 is still ongoing, but the results available so far indicate that the knowledge gained in TG4 cannot be simply be applied to the TG6 geometry and materials and achieve the same predictive accuracy.

Figure 16 compares a single, representative prediction with the measured stresses on line BD. This has the following features:

- The simulations were performed by the research team responsible for the most accurate TG4 models (see [29]), using the same FE software and the same welding heat source fitting strategy.
- The thermal solution achieved acceptable accuracy
- Parent material mechanical behaviour was described using a Lemaitre-Chaboche model fitted to representative Plate A test data using the approach developed for AISI 316.
- Weld metal mechanical behaviour was also described using a Lemaitre-Chaboche model fitted to solution-treated Alloy 82 test data, although the material was extracted from a weld pad rather than two-pass welds. No initial yield strength or hardening limit adjustments were made.
- Softening in the CGHAZ was modelled using field variables to allocate weld properties to material that exceeded a critical temperature, determined by comparing the results of microscopy and hardness mapping with the predicted maximum temperatures achieved.
- Simple “annealing” behaviour was assumed, in which the hardening history was eliminated above 1200°C.

It is evident that longitudinal stresses are generally over-predicted, especially in weld metal, the CGHAZ, and in the ligament adjacent to the HAZ, which has also reached high temperatures. In contrast, transverse stresses are consistently under-predicted. The reasons for this are not yet clear.

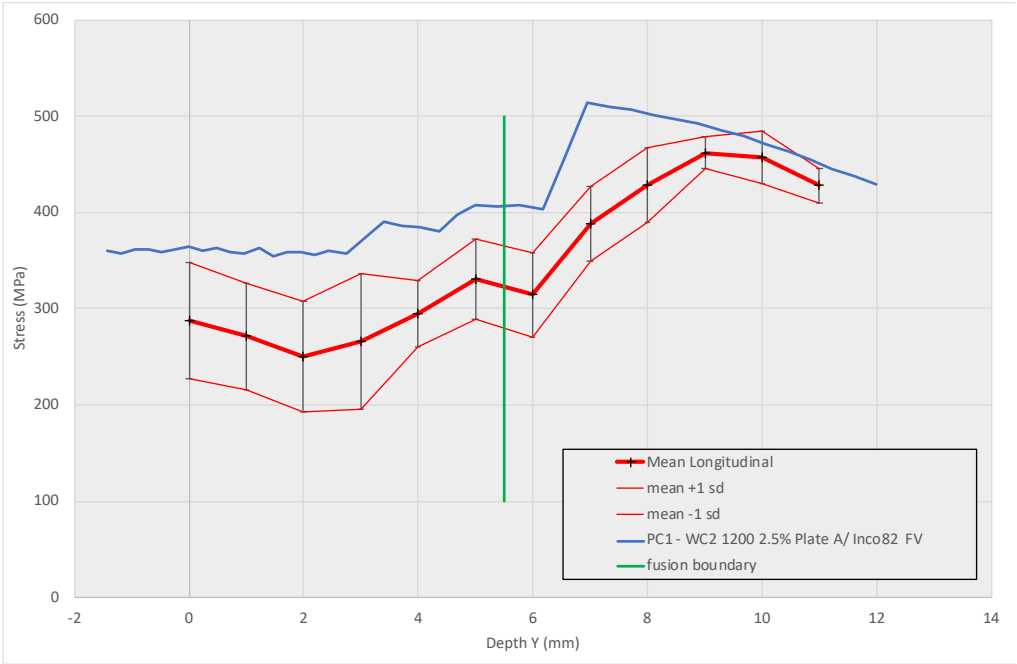

(a) Longitudinal stresses

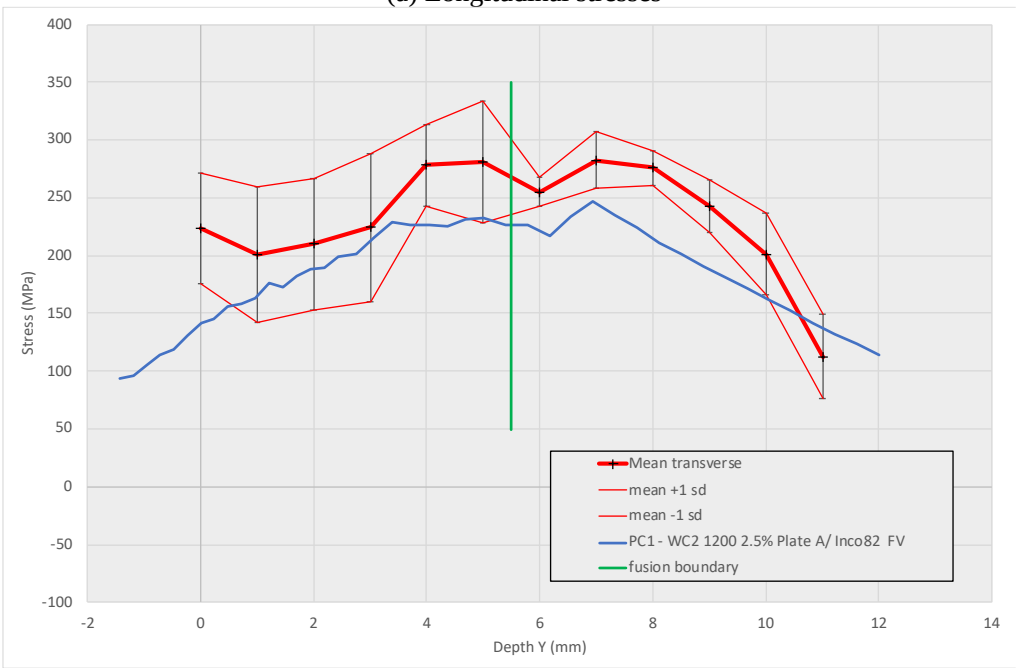

(b) Transverse stresses

Fig. 16: Comparison of predicted and measured stresses in TG6 specimen on line BD, for a single sample analysis.

DISCUSSION AND CONCLUSIONS

The end results of simulations of the welding process are quantities that are of use to engineers and scientists. The weld residual stress field is an obvious output, since this can adversely affect the service life of welds. Much of the industrial interest in weld modelling has been driven by the need to understand and manage in-service degradation of welds in nuclear powerplants, where residual stress is a key variable. Clearly there are others, such as in-process distortion or the development of important microstructural features. Whatever the desired output, the complexity of welding means that making accurate predictions is a multi-stage process, requiring validation at each stage to ensure simulations do not diverge from reality.

The NeT benchmarks reflect this need, and they offer unique test beds for the development and validation of weld simulation techniques. The plate and weld materials are thoroughly characterized, the welding conditions are well defined, and the transient thermal response is reliably characterized via redundant thermocouple arrays on multiple specimens. The weld residual stresses and accompanying structural distortions are also reliably characterized: indeed the residual stress measurements for both TG4 and TG6 are unusual in both their number and their extent.

Results from both TG4 and TG6 show that it is possible to make accurate predictions of the transient thermal fields developed during arc welding in both austenitic steels and nickel alloys. However, the scatter routinely exhibited by thermocouple measurements during welding mean that multiple specimens need to be instrumented with redundant arrays of thermocouples in order to accurately calibrate the welding heat source models. Thermocouple measurements also need to be supplemented by conventional weld metallography to establish the size and shape of the weld fusion zones.

If these data are available, then the combination of thermocouple data to calibrate "global" heat source parameters (here only the efficiency) and metallography to calibrate local heat source parameters (size and shape parameters) leads to thermal solutions with sufficient accuracy to be used for either continuum predictions of residual stresses and distortions, or indeed meso-scale predictions of microstructural features in the heat-affected zone.

Measured residual stresses are historically the most important validation measure for finite element weld models. Here the work of NeT has emphasized the need both for great care and for diversity in making such measurements. The residual stress state in NeT TG4 is known with high accuracy only because multiple diffraction-based measurements were made at multiple instruments. If only a single set of measurements had been made, then it would be a matter of "luck" whether they reflected the consensus or were an outlier[2].

Strain relief measurements show a similar pattern. In TG4 both the contour method and incremental deep hole drilling produced mixed results, and the availability of a reliable diffraction-based best estimate was an important part of the process of identifying errors in the first measurements made.

[2] Of course "luck" is not correct. It is perhaps more correct that a properly qualified team of experienced researchers should have followed best practice in making measurements at an instrument with a good track record, without being rushed by the pressure of competitive time allocation.

The validation requirements of the UK R6 procedure are shown to have a sound engineering basis: if measurements made using diffraction techniques agree well with strain relief measurements, then it is likely that an accurate estimate of the residual stresses has been made.

The first stages of the measurements round robin on NeT TG6 has served to emphasise that residual stress measurements can be made more difficult by the characteristics of the welded structure and the materials used. Neutron diffraction, as yet, has higher uncertainties than in TG4, at least partly due to the microstructural characteristics of the Alloy 600/82 welded plates. Strain relief measurements have yet to produce reliable results, probably because the characteristics of the welded plates lead to more opportunity for unwanted local plastic deformation during the measurements. Nevertheless, the NeT collaborative approach means that sufficient independent measurement data are available to identify systematic errors and outliers.

The simulation round robins performed on NeT TG4 have shown that highly accurate predictions of weld residual stress may be achieved in AISI 316L(N). However, to achieve this it is necessary to used mixed isotropic-kinematic hardening models for both weld and parent material. Simple isotropic and kinematic models lead to significant deviation from the measurements concensus. Mixed hardening models carry a significant burden of materials testing: it is necessary to perform isothermal cyclic testing over a range of temperatures up to 700°C, and monotonic tensile testing to higher temperatures, to obtain sufficient data to fit the models (those used for TG6 require 7 parameters at each temperature).

The handling of weld metal requires care. It is not acceptable to test multi-pass weld metal (its end state) in order to develop the parameters for an evolutionary hardening model. Any models fitted to multi-pass weld test data will grossly over-predict stresses in the weld metal. In TG4, weld metal testing was performed on two-pass welds (effectively a single bead due to re-melting), that had been solution-treated to remove any hardening).

Initial results for NeT TG6 indicate that approaches developed for AISI 316 may not transfer to the Alloy 600/82 combination without modification. TG6 exhibits significant under-matching, softening and re-crystallisation in the HAZ, and much higher temperatures in the ligament beneath the weld than developed in TG4. It is evident that high temperature effects, such as recovery and re-crystallisation, are more important than in TG4 where they could be ignored or handled very simply. Research to understand this and improve the accuracy of prediction continues.

AKNOWLEDGEMENTS

The NeT Network receives no external project funding. All participants in its round robin activities are either self-funded or co-funded by other participants. The authors therefore wish to acknowledge the contributions made by all the participants in NeT TG4 and NeT TG6.

Mike Smith is supported by the UK Engineering and Physical Sciences Research Council (EPSRC) Fellowship in Manufacturing “A whole-life approach to the development of high integrity welding technologies for Generation IV fast reactors”, EP/L015013/1.

Successful management of NeT collaborations requires a unique blend of skills. Until 2014, these were provided by Ann Smith. She guided the TG4 project from its inception, and was instrumental in setting up the TG6 project and guiding its participants through the early stages of the project stages. Sadly, Ann died in July 2014, shortly after being diagnosed with metastatic pancreatic cancer. She is greatly missed by all her co-workers in NeT

REFERENCES

[1] L-E LINDGREN: Finite element modeling and simulation of welding part 2: improved material modelling, J Therm Stress 24, 195-231 (2001).

[2] L-E LINDGREN: Finite element modeling and simulation of welding Part 1: increased complexity, J Thermal Stresses 24, 141-192 (2001).

[3] L-E LINDGREN: Computational welding mechanics. Thermomechanical and microstructural simulations, Cambridge, Woodhead Publishing Ltd (2007).

[4] R6, Assessment of the integrity of structures containing defects, EDF Energy (2015).

[5] Fitness for Service, API 579-1/ASME FFS-1, Second Edition (2007).

[6] P HURRELL, C WATSON, P J BOUCHARD, M C SMITH, R J DENNIS, N A LEGGATT, S K BATE and A WARREN: Development of weld modelling guidelines in the UK, ASME PVP 2009, Prague, PVP2009-77540 (2009).

[7] S BATE and M SMITH: Determination of residual stresses in welded components by finite element analysis, Materials Science and Technology 32(14), 1505-1516 (2016).

[8] C E TRUMAN and M C SMITH: The NeT residual stress measurement and analysis round robin on a single weld bead-on-plate specimen, Int Jnl Press Vess and Piping 86(1), 1-2 (2009).

[9] M C SMITH and A C SMITH: NeT bead on plate round robin: Comparison of transient thermal predictions and measurements, Int Jnl Press Vess and Piping 86(1), 96-109 (2009).

[10] M C SMITH and A C SMITH: NeT bead on plate round robin: Comparison of residual stress predictions and measurements, Int Jnl Press Vess and Piping 86(1), 79-95 (2009).

[11] X FICQUET, D J SMITH, C E TRUMAN, E J KINGSTON and R J DENNIS: Measurement and prediction of residual stress in a bead-on-plate weld benchmark specimen, Int Jnl Press Vess and Piping 86(1), 20-30 (2009).

[12] M C SMITH, B NADRI, A C SMITH, D G CARR, P J BENDEICH and L EDWARDS: Optimisation of mixed hardening material constitutive models for weld residual stress simulation using the NeT Task Group 1 single bead on plate benchmark problem, ASME PVP 2009, Prague, PVP2009-77158 (2009).

[13] P J BENDEICH, M C SMITH, D G CARR and L EDWARDS: Sensitivity of predicted weld residual stresses in the NeT Task Group 1 single bead on plate benchmark problem to finite element mesh design and heat source characteristics, ASME PVP 2009, Prague, PVP2009-77584 (2009).

[14] M C SMITH, A C SMITH, R WIMPORY and C OHMS: A review of the NeT Task Group 1 residual stress measurement and analysis round robin on a single weld bead-on-plate specimen, Int Jnl Press Vess and Piping 120–121(0), 93-140 (2014).

[15] P J BOUCHARD: The NeT bead on plate benchmark for weld residual stress simulation, Int Jnl Press Vess and Piping 86(1), 31-42 (2009).

[16] P GILLES, W EL-AHMAR and J-F JULLIEN: Robustness analyses of numerical simulation of fusion welding NeT-TG1 application: "single weld-bead-on-plate", Int Jnl Press Vess and Piping 86(1), 3-12 (2009).

[17] M HOFFMAN and R C WIMPORY: NeT TG1:Residual stress analysis on a single bead weld on a steel plate using neutron diffraction at the new engineering instrument "STRESS-SPEC", Int Jnl Press Vess and Piping 86(1), 122-125 (2009).
[18] R M MOLAK, K PARADOWSKI, T BRYNK, L CIUPINSKI, Z PAKIELA and K J KURZYDLOWSKI: Measurement of mechanical properties in a 316L stainless steel welded joint, Int Jnl Press Vess and Piping 86(1), 43-47 (2009).
[19] C OHMS, R C WIMPORY, D E KATSAREAS and A G YOUTSOS, NET TG1: Residual stress assessment by neutron diffraction and finite element modellng on a single weld on a steel plate, Int Jnl Press Vess and Piping 86(1), 63-72 (2009).
[20] S PRATIHAR, M TURSKI, L E EDWARDS and P J BOUCHARD: Neutron diffraction residual stress measurements in a 316L stainless steel bead-on-plate weld specimen, Int Jnl Press Vess and Piping 86(1), 13-19 (2009).
[21] X SHAN, C M DAVIES, T WANGSDAN, N P O'DOWD and K M NIKBIN: Thermo-mechanical modelling of a single-bead-on-plate weld using the finite element method, Int Jnl Press Vess and Piping 86(1), 110-121 (2009).
[22] M TURSKI and L E EDWARDS: Residual stress measurements of a 316L stainless steel bead-on-plate specimen utilising the contour method, Int Jnl Press Vess and Piping 86(1), 126-131 (2009).
[23] R C WIMPORY, C OHMS, M HOFFMAN, R SCHNEIDER and A G YOUTSOS: Statistical analysis of residual stress determination using neutron diffraction, Int Jnl Press Vess and Piping 86(1), 48-62 (2009).
[24] K ABBURI VENKATA, C E TRUMAN, R C WIMPORY and T PIRLING: Numerical simulation of a three-pass TIG welding using finite element method with validation from measurements, Int Jnl Press Vess and Piping 164, 68-79 (2018).
[25] L DEPRADEUX and R COQUARD: Influence of viscoplasticity, hardening, and annealing effects during the welding of a three-pass slot weld (NET-TG4 round robin), Int Jnl Press Vess and Piping 164, 39-54 (2018).
[26] O MURÁNSKY, C J HAMELIN, F HOSSEINZADEh and M B PRIME, Evaluation of a self-equilibrium cutting strategy for the contour method of residual stress measurement, Int Jnl Press Vess and Piping 164, 22-31 (2018).
[27] O Muránsky, F Hosseinzadeh, C J Hamelin, Y TraoRE and P J BENDEICH, Investigating optimal cutting configurations for the contour method of weld residual stress measurement, Int Jnl Press Vess and Piping 164, 55-67 (2018).
[28] O MURÁNSKY, M TRAN, C J HAMELIN, S L SHRESTHA and D BHATTACHARYYA, Assessment of welding-induced plasticity via electron backscatter diffraction, Int Jnl Press Vess and Piping 164, 32-38 (2018).
[29] M C SMITH, O MURÁNSKY, C AUSTIN, P BENDEICH and Q XIONG, Optimised modelling of AISI 316L(N) material behaviour in the NeT TG4 international weld simulation and measurement benchmark, Int Jnl Press Vess and Piping 164, 93-108 (2018).
[30] M C SMITH and A C SMITH, Advances in weld residual stress prediction: A review of the NeT TG4 simulation round robins part 2, mechanical analyses, Int Jnl Press Vess and Piping 164, 130-165 (2018).
[31] M C SMITH and A C SMITH, Advances in weld residual stress prediction: A review of the NeT TG4 simulation round robin part 1, thermal analyses, Int Jnl Press Vess and Piping 164, 109-129 (2018).
[32] M C SMITH, A C SMITH, C OHMS and R C WIMPORY, The NeT Task Group 4 residual stress measurement and analysis round robin on a three-pass slot-welded plate specimen, Int Jnl Press Vess and Piping 164, 3-21 (2018).
[33] R C WIMPORY, R V MARTINS, M HOFMANN, J R KORNMEIER, S MOTURU and C OHMS, A complete reassessment of standard residual stress uncertainty analyses using neutron

diffraction emphasizing the influence of grain size, Int Jnl Press Vess and Piping 164, 80-92 (2018).
[34] M C SMITH, S K BATE and P J BOUCHARD, Simple benchmark problems for finite element weld residual stress simulation, ASME Pressure Vessels and Piping Conference, Paris, PVP2013-98033 (2013).
[35] C J HAMELIN, O MURÁNSKY, M C SMITH, T M HOLDEN, V LUZIN, P J BENDEICH and L EDWARDS, Validation of a numerical model used to predict phase distribution and residual stress in ferritic steel weldments, Acta Materialia 75(0), 1-19 (2014).
[36] H J RATHBUN, D RUDLAND, L FREDETTE, A CSONTOS and P SCOTT, NRC welding residual stress validation program – International round robin details and findings, 2011 ASME Pressure Vessels and Piping Division Conference, Baltimore, 17th-20th July 2011, PVP 2011-57642 (2011).
[37] L FREDETTE, M KERR, H J RATHBUN and J E BROUSSARD, NRC/EPRI Welding Residual Stress Validation Program - Phase III Details and Findings, ASME Pressure Vessels and Piping Conference, Baltimore, PVP2011-57645 (2011).
[38] O MURANSKY, M C SMITH, P J BENDEICH and L EDWARDS, Validated numerical analysis of residual stresses in Safety Relief Valve (SRV) nozzle mock-ups, Computational Materials Science 50(7), 2203-2215 (2011).
[39] P J BENDEICH, O MURANSKY, C J HAMELIN, M C SMITH and L EDWARDS, Validated numerical analysis of residual stresses in safety relief valve (SRV) nozzle mock-ups: influence of axial restraint on distortion and residual stress predictions, Computational Materials Science 62, 285-288 (2012).
[40] M C SMITH and O MURANSKY, The NeT task group 6 weld residual stress measurement and simulation round robin in alloy 600/82, ASME Pressure Vessels and Piping Conference, Vancouver, PVP2016-63941 (2016).
[41] M TURSKI, M C SMITH, P J BOUCHARD, L EDWARDS and P J WITHERS, Spatially resolved materials property data from a uniaxial cross-weld tensile test, Journal of Pressure Vessel Technology 131(6), (2009).
[42] M C SMITH, P J BOUCHARD, M TURSKI, L EDWARDS and R J DENNIS, Accurate prediction of residual stress in stainless steel welds, Computational Materials Science 54, 312-328 (2012).
[43] O MURANSKY, M C SMITH, P J BENDEICH, T M HOLDEN, V LUZIN, R V MARTINS and L EDWARDS, Comprehensive numerical analysis of a three-pass bead-in-slot weld and its critical validation using neutron and synchrotron diffraction residual stress measurements, International Journal of Solids and Structures 49(9), 1045-1062 (2012).
[44] F HOSSEINZADEH, Y TRAORE, P J BOUCHARD and O MURÁNSKY, Mitigating Cutting-Induced Plasticity in the Contour Method, Part 1: Experimental, International Journal of Solids and Structures.